The literature survey reveals that several organic compounds containing hetero atoms like boron [V. Jaiswal et al. (2014)], oxygen, nitrogen [Wan et al. (1997), Li et al. (2000), He et al. (2002), Qaio et al. (2011), Yang et al. (2013)], halogens, sulphur [Biresaw et al. (2004)] and phosphorus [Najman et al. (2004a), Najman et al. (2004b), Mangolini et al. (2009)] etc. have been extensively used as multifunctional additives like antiwear, extreme pressure [Kim et al. (2011)], antioxidant and corrosion inhibitor in lubricating oil. Basically, the antiwear and friction reducing additives get physically and/ or chemically adsorbed on the interacting surfaces through different adsorption centres like hetero atoms, phenyl rings and double bonds etc. Thus, *in situ* generated chemical film, formed through the process of adsorption prevents proximity of the contact surfaces. Consequently, the friction and wear are reduced [Shah et al. (2009a), Bhushan et al. (1995), Didziulis et al. (1995) Lara et al. (1998)]. Numerous literature reports [Cavdar et al. (1991), Mosey et al. (2003), Willermet et al. (1992)] are available where surface characterization techniques have provided adequate evidence in favour of the adsorption film. The performance of additives depends on the various factors such as polarity of functional group, composition and chemical activity of metal surfaces.

The quantification of structure-activity relationship of wear and friction modifiers is important as it may help in designing the lubricant additives depending on the requirement of the system. Recently Quantum Chemical Calculations based on Density Functional Theory, have been used to correlate structure and triboactivity [Shenghua et al. (2004), Jaiswal et al. (2014)]. As mentioned earlier, adsorption centres (like phenyl groups, heteroatoms etc.) in these large additive molecules play a critical role in determining their lubricating properties. Therefore, a large number of recent

quantum mechanical studies are limited to studying the interaction between the key functional groups of the additive molecule and small cluster or unit cells of the surface material. However, it is not possible to explicitly include a solvent or the dispersing medium molecules in such investigations. Vital questions, like nature and mechanism of adsorption of such large additive molecules in the presence of dispersing medium molecules, remain unanswered. Even the configuration of these large additive molecules, after being adsorbed, is largely unknown. Molecular dynamics (MD) simulations on adsorption of the additive molecules on the surface, typically in the explicit presence of dispersing medium molecules, can provide important information required for understanding the mechanism of the mentioned adsorption problem [T. Ta et al. (2017a)]. Moreover, the knowledge of the conformation of the additive molecule after its adsorption on the adsorbent is critical for developing the mechanism of triboactivity of these molecules [T. Ta et al. (2015)].

Organic compounds containing heteroatoms, oxygen and nitrogen-containing friction modifiers capture the scene being environmentally benign from the tribological perspective as these do not poison the efficiency of catalytic converters used in engine exhaust after-treatment systems [Hertley et al. (2002), Devid et al. (2002)]. In this category of compounds, Schiff bases [Jaiswal et al. (2015) Rastogi et al. (2014), Jaiswal et al. (2013)] synthesized from the condensation reaction between -CHO and $–NH_2$ functional groups of the reacting species, have been extensively studied. These biologically active molecules are commonly used as antitumor, antibacterial and antifungal drugs [Samanta et al. (2007), Anacona et al. (1999), Golcu et al. (2005)]. Besides biological activity, these are reported for their antiwear, antioxidant and anticorrosive properties also [Singh et al. (2015) (2016a)].

This chapter presents syntheses of different Schiff bases of *o*-tolidine with salicylaldehyde (OH-BT), naphthaldehyde (H-NT) and 2-hydroxynaphthaldehyde (OH-NT), characterization by FT-IR, ^{1}H NMR spectroscopic techniques and evaluation of their tribological behavior in paraffin oil using four-ball tester. The synthesized Schiff bases are expected to exhibit appreciable tribological behavior owing to the presence of triboactive centers like, -OH, -CH=N- and phenyl ring. Participation of the imine group has been adjudged by a drastic decrease in the antiwear activity of OH-BTS (the product of the reaction of OH-BT with thioglycolic acid) where imine groups have disappeared. Surface characterization of the interacting tribo- pairs has been achieved by the Scanning electron microscopy (SEM), Atomic force microscopy (AFM). For fortuitous development in the field of lubrication technology, the understanding of the mechanism of tribological behavior at the atomic level is difficult to achieve experimentally. Molecular dynamics simulations, therefore, were finally used to study the mechanism of adsorption of the studied Schiff bases in paraffin oil on the iron slab. The order of adsorption energies of the Schiff base additive molecules and the nature of orientation or configuration after adsorption have been presented. This understanding has been used to propose a mechanism of additive action for the investigated Schiff base molecules.

3.1. Materials & methods

3.1.1. Chemicals

All chemicals, *o*-tolidine, salicyldehyde, naphthaldehyde, 2-hydroxy-naphthaldehyde, glacial acetic acid, sodium bicarbonate and solvents were of analytical grade and were used as received. The solvent *n*-hexane used for cleaning the specimen

was obtained from Fisher Scientific Co. (Mumbai, India). Zinc dialkyldithiophosphate (ZDDP) was procured from Flexsys Chemicals (M) SdnBhd, U.S.A. and used as reference additive.

3.1.2. Synthesis

For the synthesis of Schiff bases, ethanolic solution of *o*-tolidine (10 mmol) was added to the ethanolic solution (20 mmol) of the aldehyde [salicyldehyde/ naphthaldehyde/ 2-hydroxy- naphthaldehyde]. The reaction mixture was refluxed for 5-8 h with constant stirring after addition of 1-2 drops of glacial acetic acid. The progress of the reaction was followed by thin-layer chromatography (TLC). After completion of the reaction, the reaction mixture was cooled at room temperature. The precipitate appeared was filtered, washed with distilled water.

Scheme 1. Synthesis of Schiff base OH-BT via condensation of salicylaldehyde with *o*-tolidine

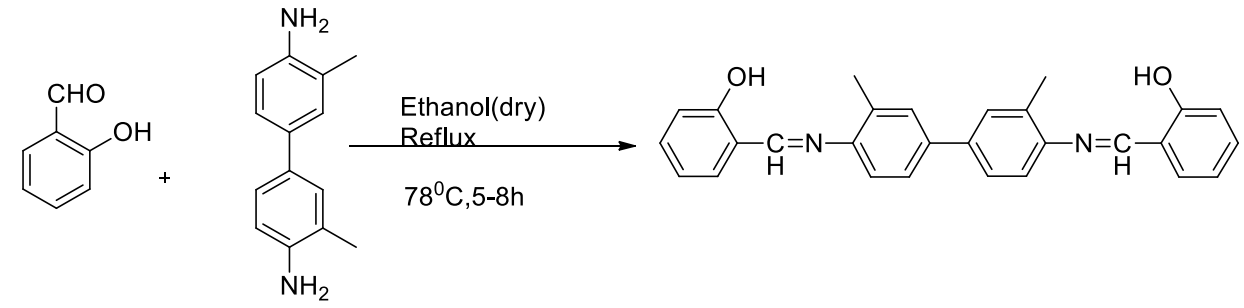

Salicylaldehyde **o-tolidine** **OH-BT**

In a reaction flask Schiff base OH-BT (1 mmol) and thioglycolic acid (2.05 mmol) were mixed in toluene (10 ml) and refluxed for eight to twelve hours. After completion of the reaction, as confirmed by TLC, the reaction mixture was cooled to room temperature. The solvent was evaporated, and the solid product was washed with

aqueous $NaHCO_3$ solution to remove the excess of thioglycolic acid followed by ethanol. It was then dried *in vacuo* [Mutahir et al. (2017)].

Scheme 2. The reaction of Schiff base OH-BT with thioglycolic acid yielding OH-BTS

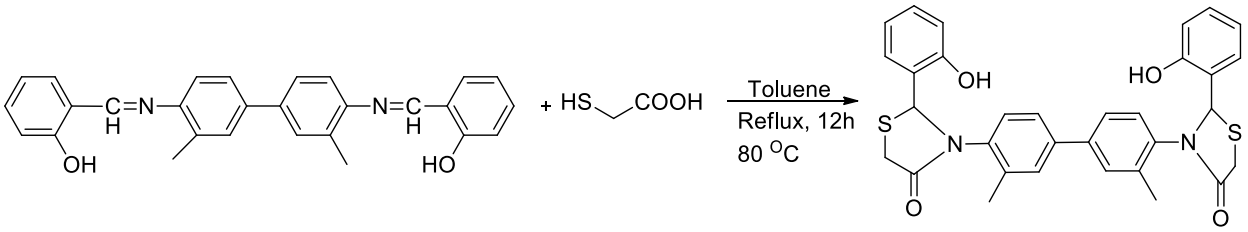

OH-BT **Thioglycolic acid** **OH-BTS**

IUPAC names, structures, and abbreviations of synthesized additives are presented in **Table 3.1**

All the synthesised compounds have been characterized by infrared and proton nuclear magnetic resonance spectroscopic techniques.

Table 3.1. IUPAC names, structures and abbreviations of synthesized additives

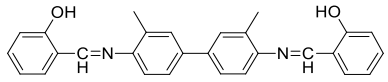	2,2'[(3,3'dimethyl-[1,1'] biphenyl]4,4'diyl)bis(azanylylidene) bis(methanylylidene) diphenol	OH-BT
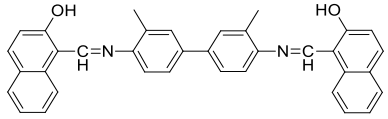	1,1'[(3,3'dimethyl-[1,1'] biphenyl] 4,4'diyl) bis(azanylylidene)bis (methanylylidene) bisnaphthalene-2-ol	OH-NT
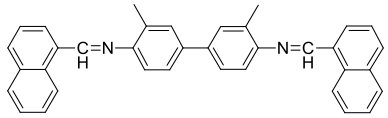	3,3'dimethyl-N, N-(bis (naphthalene-1 -yl methylene)-[1,1'-biphenyl]-4,4'diamine	H-NT
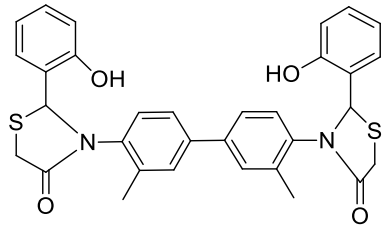	3,3'-(3,3'-dimethyl-[1,1'-biphenyl]-4,4-diyl) bis(2-(2-hydroxyphenyl) thiazolidine-4-one	OH-BTS

3.2. Tribological Characterization

3.2.1. Lubricant Sample Preparation

Uniform suspensions of paraffin oil with reference additive ZDDP and Schiff base additives in different concentrations 0, 0.125, 0.25, 0.5, 1 % (w/v) were prepared by stirring for 1-2 h on the magnetic stirrer. The optimum concentration for the additives was found to be 0.25% w/v, and all tests were, therefore, performed at this concentration. The balls of AISI 52100 alloy steel of 12.7 mm diameter (hardness 59-61 HRc) were used for the tests. Steel balls were washed with n-hexane and rigorously air-dried before and after the test.

3.3. Computational Methodology

All models were constructed using the Materials and Processes Simulations Platform (MAPS version 4.0.1) from Scienomics SARL (Paris, France). The molecules required for making the four model systems were constructed using the MAPS molecule builder. Each molecule (OH-BT, OH-BTS, OH-NT, H-NT) in paraffin oil was first constructed by the MAPS molecular builder and then geometrically optimized by MNDO [Dewar et al. (1977)]. The configurations of the geometrically optimized Schiff molecules considered in the present study is given in Figure. All molecules making the paraffin oil (PO), were modeled as a linear chain of alkanes consist of 56 atoms [$C_{18}H_{38}$]. The BCC Fe unit cell was used to construct the supercell, and then this was cleaved to obtain its (110) surface. The Fe (110) surface slab dimensions thus obtained were approximately 42.90Å × 42.90 Å×8.58 Å. Fe (110) surface slab was placed normal to the z-axis of the simulation cell. It makes up one end of the rectangular simulation cell. Overall dimensions of the simulation box were 42.90Å × 42.90 Å×681.48Å. The space

that is empty after the Fe (110) slab along the z-direction is the vacuum gap. Such large vacuum gap along the z-direction was taken to remove the interactions between periodic images in the z-direction.

The initial input model configuration for the MD simulation was made in the following way. One OH-BT (adsorbate) molecule was dispersed into eighteen paraffin oil molecules (1:18 ratio) by using the amorphous builder in MAPS 4.1. These molecules were placed adjacent to the Fe (110) slab surface at an appropriate initial density. The atoms making up the Fe (110) were not fixed and owing to thermal noise they were vibrating (about their mean positions) throughout the simulation. The adsorbate and dispersion medium configuration was subjected to initial optimization by the conjugate gradient approximation approach. This model is henceforth denoted as system A in the rest of the manuscript.

The other three models for OH-BTS, H-NT and OH-NT molecules in paraffin oil were also constructed in the same way as system A. PCFF force field (given in MAPS 4.1) was applied on these models. The non-bonded interactions between Fe atoms and adsorbate/PO molecules were modeled by the 9−6 potential Lennard-Jones (LJ) potential in the PCFF force field [Plimpton et al. (1995)]. The PCFF force field used was modified by adding Fe-C and Fe-H LJ interaction parameters from reference [Ta et al. (2015)] for these simulations. The function below gives the van der Waal part of the PCFF force field.

$$\mathbf{U_{LJ}} = \varepsilon[\ \mathbf{2}\left(\frac{\sigma}{r_{min}}\right)^{\mathbf{9}} - \mathbf{3}\left(\frac{\sigma}{r_{min}}\right)^{\mathbf{6}}] \qquad 3.1$$

In the above function ε is the well-depth, σ is van der Waals radii, r_{min} is the distance between atom type.

Each model was subjected to molecular dynamics (MD) simulation in the NVE ensemble for 20 nanoseconds using a time step of 1 femtosecond. Coulomb interactions were simulated with the particle mesh approach using a cut off distance of 12 Å. The initial temperature was T = 298.15 K. LAMMPS [Wilburn et al. (1978)] program was used to run the MD simulations. The potential energy of adsorption of the adsorbate molecules on to the Fe (110) surface in the presence of dispersing medium was calculated in the following way. Results of the interacting models mentioned above were compared with non-interacting simulation or reference model. The reference model potential energy was the sum of equilibrium (long-time average) energies of the separate system of solute molecules only, the bare slab system and separate system of solvent molecules. Simulations for all component reference models were also run for 20 nanoseconds under identical NVE ensemble conditions.

3.4. Results and discussion

3.4.1. Antiwear and anifriction properties

The mean wear scar diameter (MWD) is a measure of the degree of wear under sliding contact. **Fig. 3.1** illustrates the relation between MWD and concentration of additives in the PO at 392 N applied load. It can be seen from the figure that MWD values are reduced remarkably in the presence of the additives at all concentrations as compared to PO. Thus, all of them may be employed as good antiwear additives at the steel-steel interface. With an increase in concentration from 0.00 to 0.25% w/v, MWD values decrease successively in every case. After that, MWD increases appreciably in each

case up to 0.50% w/v. Beyond this, MWD values decrease slightly to 1% concentration. Thus, the lowest value of MWD was perceived at 0.25% (w/v) concentration for each of the synthesized additive. Therefore, all tribological tests were performed at this concentration. The MWD data of the additives at the optimized concentration, 0.25% indicate a phenomenal reduction in the presence of admixtures as compared to blank oil (0.733 mm), OH-BT (0.525), OH-NT (0.541) and H-NT (0.580). It is a noticeable observation that in the case of ZDDP, best results are obtained at 1% concentration. Therefore, ZDDP is not a good additive at all at low concentrations.

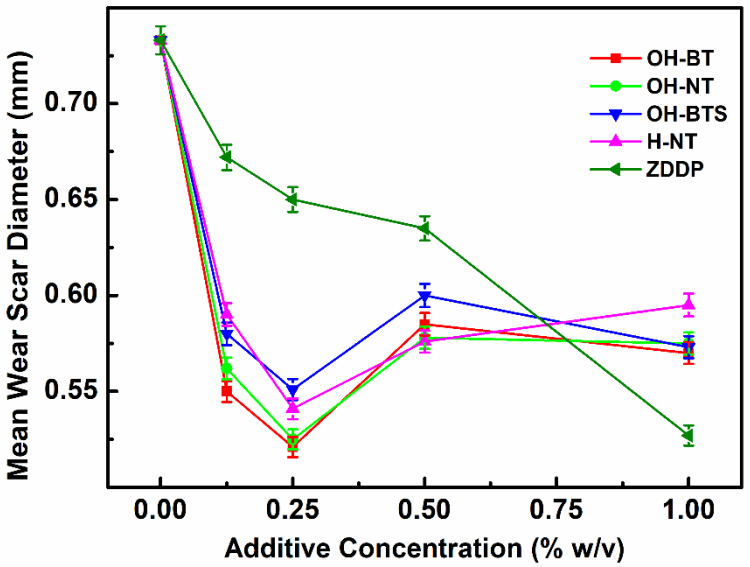

Fig. 3.1. Variation of mean wear scar diameter as a function of additive concentration (392 N, 60 min)

The friction reduction was studied at the optimized concentration to see the relative performance of different additives. **Fig. 3.2** displays alteration in the coefficient of friction (COF) with time in blank oil and oil blended with additives (0.25% w/v) at applied load 392N for 60 min test period. It is conspicuous from the figure that maximum reduction in COF values is observed for OH-BT followed by OH-NT, then

H-NT and finally ZDDP. **Fig. 3.3** exhibits a remarkable reduction in MWD and COF values together in the presence of the synthesized additives along with reference additive ZDDP. Thus, the same order of activity is inferred from both MWD and coefficient of friction data.

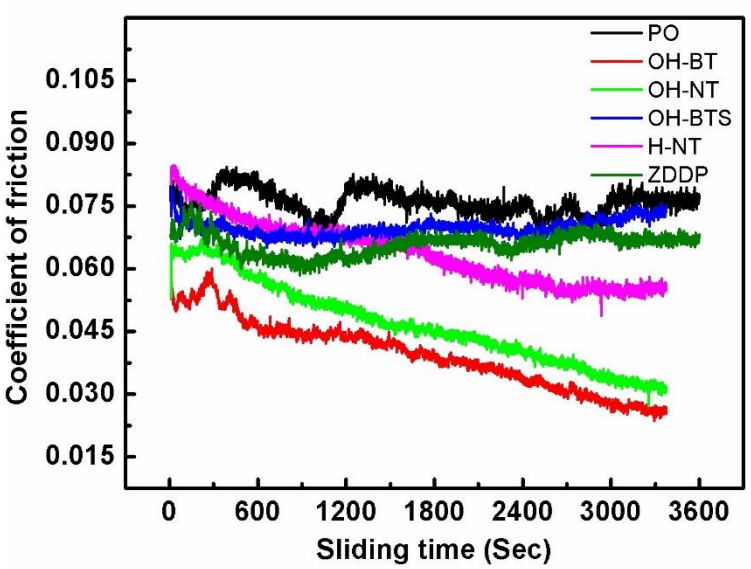

Fig. 3.2. Variation of coefficient of friction as a function of sliding time in paraffin oil with and without different antiwear additives (0.25 % w/v) at 392N applied load for 60 min test duration

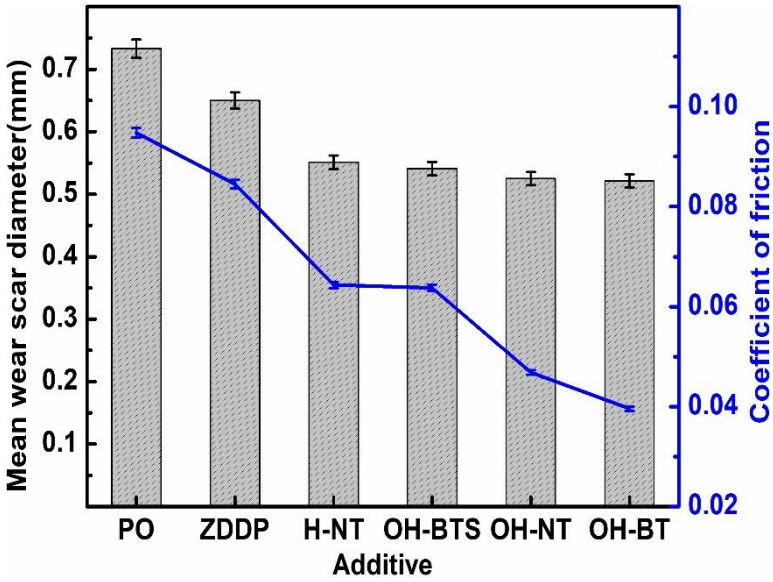

Fig. 3.3. Comparative analysis of wear scar diameter and coefficient of friction (COF) of different additives at an optimum concentration of 0.25% (w/v) in paraffin oil (392 N, 60 min)

The observed antiwear performance of the studied Schiff bases can be explained based on their structures. The number of heteroatoms/aromatic rings/the donor groups and planarity of the molecule are some of the factors which affect the efficiency of an antiwear additive. Larger the surface area, higher the number of heteroatoms/aromatic rings/ and donor groups, greater is the tendency of the additive to form film via adsorption on the steel surface [Cavdar et al. (1998)].

The activity of the investigated Schiff bases may be ascribed to their adsorption through the imine group along with other active sites like phenyl, naphthyl, methyl and hydroxyl groups [Jaiswal et al. (2015)]. To see the role of the imine group in adsorption of Schiff bases, the reaction of the most active compound OH-BT was performed with thioglycolic acid in toluene for 12 hours. The reaction product (OH-BTS) shows cyclization of the thioglycolic group with imine. As a result, the imine group -CH=N-

has disappeared and a single bond is formed in its place. A comparison of The MWD and COF values of OH-BTS were found to show a substantial increase from those of OH-BT (**Fig. 3.2 and 3.3**). This evidence is conclusive towards the involvement of imine group in adsorption of a Schiff base over the metal surface resulting into formation of tribofilm dedicated to reducing friction and wear.

Out of three Schiff bases, OH-BT is derived from salicylaldehyde while the remaining two are naphthaldehyde derivatives. Since the aromaticity of naphthyl group is lesser than that of phenyl group due to decreased delocalization of electrons, adsorption of the additive through naphthyl group is lesser (OH-NT and H-NT) as compared to that of the phenyl group in OH-BT. Out of OH-NT and H-NT, -OH group is supposed to facilitate adsorption more actively in comparison with -H of H-NT. Given the above, the observed order of MWD and COF can be directly correlated with the capability of the additive to get adsorbed over the mating surface:

OH-BT > OH-NT > H-NT

3.4.2. Wear rate

Antiwear tests were also performed for paraffin oil and its blends with additives for various periods 0.25, 0.50, 0.75, 1, 1.25 and 1.50 h at 392 N applied load to determine wear rate. Table S1 from the observed MWD, mean wear volume (MWV) was calculated as it is the more appropriate term for determination of wear rate [Jaiswal et al. (2014)]. **Fig. 3.4** depicts the behavior of MWV with time at 392 N load in the presence of admixtures. Overall wear rate was determined by fitting a linear regression model using origin and the other points. As expected, the overall wear rate was

observed to be very high for plain oil, and it decreased in the order of increasing antiwear efficiency of the studied additives.

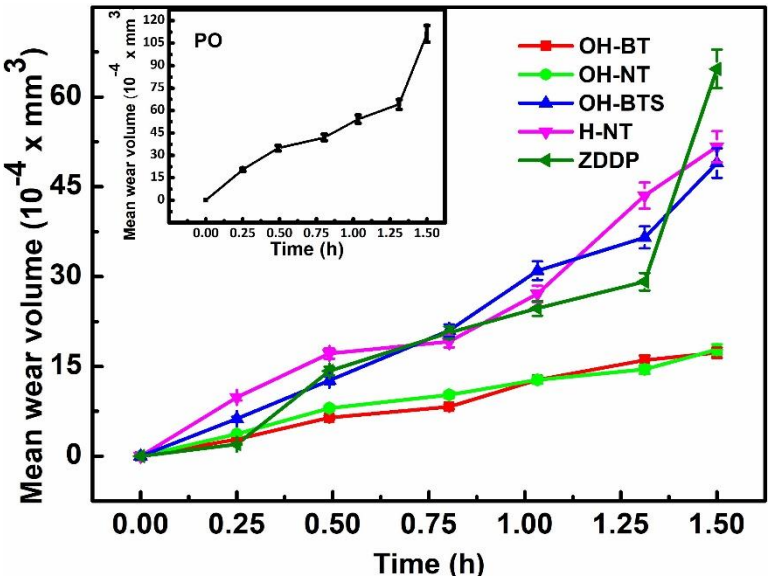

Fig. 3.4. Variation of mean wear volume of various additives with time at an optimum concentration of 0.25% (w/v)

The running-in wear rate is believed to be always higher than steady-state wear rate since initial surface changes are to be accommodated during running-in wear. After the steady-state, wear is almost stabilized. For a good antiwear additive, it is important to attain steady state at the earliest and retain it for a longer period as it is directly related to the longevity of mechanical parts of a machine [Syahn et al. (2006)]. The values of overall, running-in and steady-state wear rates in the presence and absence of the additives collected in **Table 3.2**, lie in the following order:

PO > H-NT > OH-BTS > OH-NT > OH-BT

The order can be convincingly justified given the corresponding antiwear properties.

Table 3.2. Wear-rate for PO in the presence and absence of additive for 60 min test duration at 392 N applied load

S.N.	Lubricants	Wear rate (10^{-4} x mm^3/h)	
		Running-in	Steady-state
1	OH-BT	12.93	1.6
2	OH-NT	16.05	2.1
3	OH-BTS	34.30	3.3
4	H-NT	25.32	6.1
5	ZDDP	29.41	22.78
6	PO	69.99	38.88

3.4.3. Effect of load

The load-carrying capability of the synthesized additives was evaluated through the load ramp test. The test was performed at 600 rpm according to ASTM D5183 norms. In this test, frictional torque is recorded by varying the load starting from 98 N and adding an extra 98N after every 10 min of test run. **Fig. 3.5** represents the correlation of frictional torque (T_f) with time at subsequent loads starting from 98 N. For plain paraffin oil T_f increases very slowly up to 980 N. A sudden increase in frictional torque is observed when the load is increased from 980 N to 1078 N. However, in case of admixtures the abrupt increase in frictional torque is observed at much higher loads; OH-BT (2744 N), OH-BTS (2156 N), OH-NT (2646 N), H-NT (2058 N). Accordingly, the best antiwear and friction-reducing additive OH-BT exhibits maximum load

carrying ability while additive H-NT possessing lowest friction and wear-reducing properties shows minimum load-carrying ability, too.

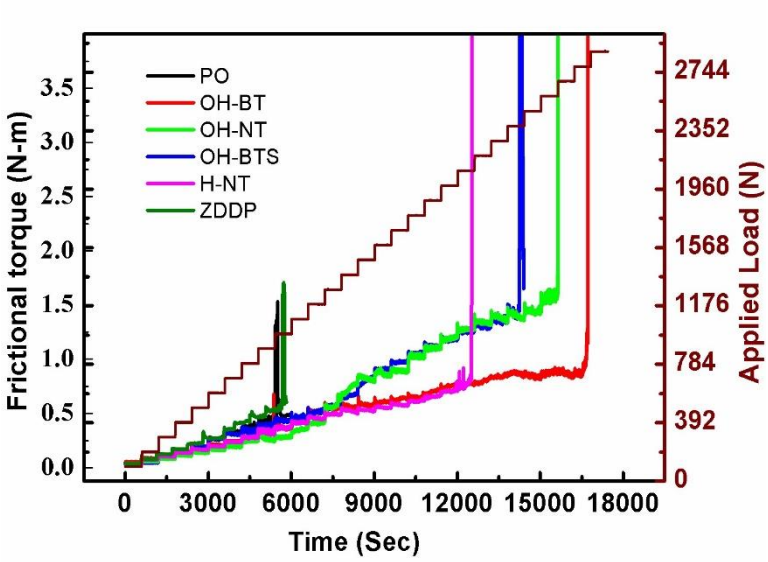

Fig. 3.5. Variation of frictional torque with time and step loading of 98 N after every 10 min of the test run for the optimized concentration (0.25 %w/v) of different additives

3.4.4. Surface Characterization

3.4.4.1. Surface morphology

The surface morphology of the wear scar has been investigated by scanning electron microscopy (SEM) and atomic force microscopy (AFM). **Fig. 3.6** exhibits worn surface of steel ball lubricated with plain paraffin oil and its admixtures (0.25 % w/v) at 392 N applied load for 60 min test duration. The surface is severely damaged when it is paraffin oil alone. On the other hand, smoothness is significantly improved in the presence of additives; it is, of course, marvellous improvement in the presence of OH-BT. The degree of smoothness due to different additives follows the same order as that of antiwear properties and relates well with the experimentally observed running -in wear rate.

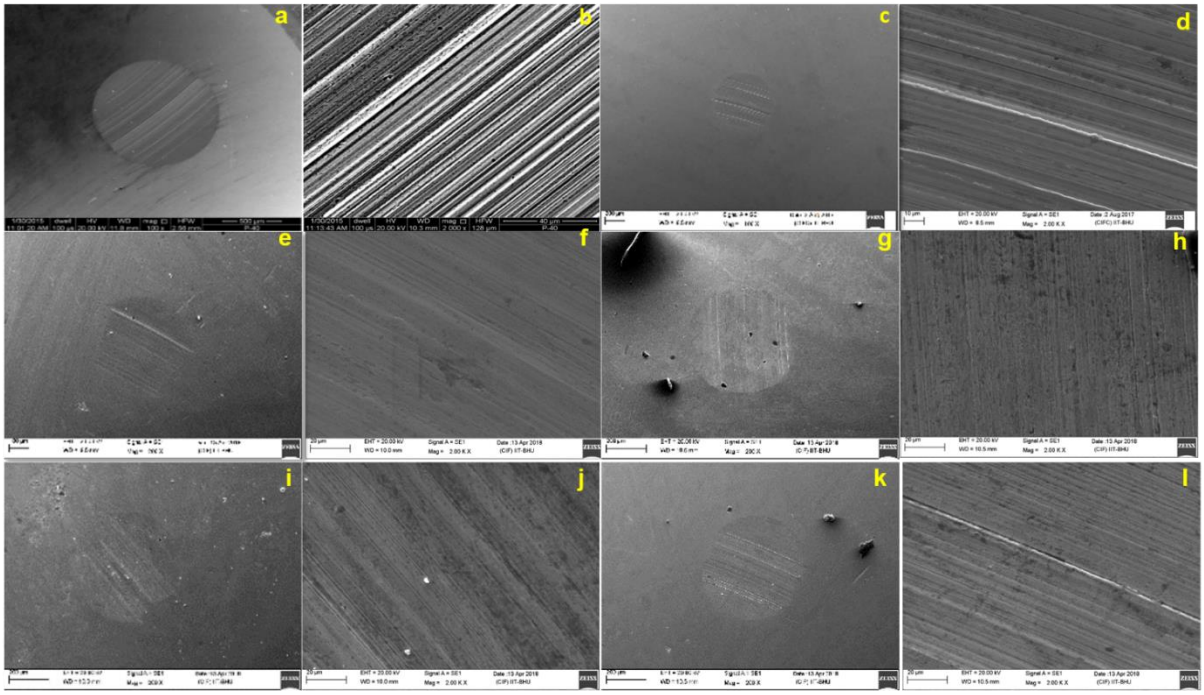

Fig. 3.6. SEM micrographs (magnification 200X and 2.00kX) of the worn surface of steel ball in the presence of base oil and its admixtures (a, b) PO, (c, d) ZDDP, (e, f) OH-BT, (g, h) OH-BTS, (i, j) OH-NT, (k, l) H-NT at 392 N load 60 min test duration

The surface roughness of the worn surface of steel ball lubricated with paraffin oil with and without additives OH-BT, OH-BTS, H-NT, OH-NT and ZDDP after the antiwear test performed at 392 N applied load for 60 min duration, was analysed by contact mode atomic force microscopy. **Fig. 3.7** displays *2D* and *3D*-AFM images and corresponding line profile graphs of the wear scar. The peaks and valleys are visible in *3D* images. The difference between their heights may be directly related to surface irregularity. The difference in heights is observed to be very large in the case of paraffin oil alone. However, in the presence of additives, the difference is drastically reduced. The irregularity of the surface is measured in terms of root mean square area roughness (S_q) and line roughness (R_q). It is apparent that in the case of paraffin oil alone, the values of these parameters are very high, 537 nm and 556 nm respectively, which are

greatly diminished when additives are present. In the presence of the best antiwear additive OH-BT these values are observed at 27.56 and 36.21 nm respectively while the product of its reaction with thioglycolic acid, OH-BTS shows them as 63.15 and 72.42 nm respectively. This observation again confirms that the activity of the additive OH-BT has substantially decreased after the reaction with thioglycolic acid. Moreover, roughness parameters support very well the experimental order of antiwear behavior of the studied additives. The decrease in surface roughness is, of course, due to tribofilm formed by the additive adsorbed over the metal surface.

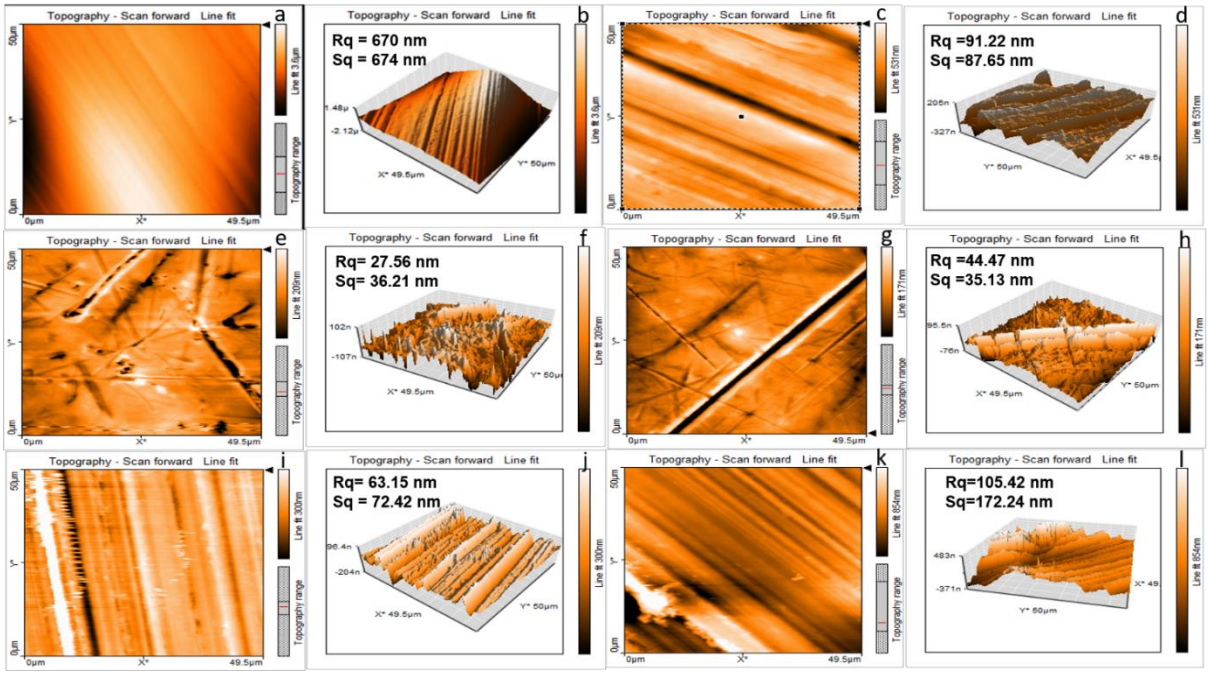

Fig. 3.7. *2D* and *3D* AFM images of the worn steel surface lubricated with different additives in paraffin oil for 60 min test duration at a 392 N applied load (a, b) PO, (c, d) ZDDP, (e, f) OH-BT, (g, h) OH-NT, (i, j) OH-BTS, (k, l) H-NT

3.4.4.2. Chemical analysis of tribofilm

For determination of the elemental composition of the tribofilm formed during ASTM D4172 test, EDX spectra of the worn surface of steel ball lubricated with paraffin oil and its admixtures with different additives have been recorded, **Fig. 3.8**. The spectrum of worn surface lubricated with OH-BT exhibits peaks due to oxygen and nitrogen while peak attributed to S is evident in the case of the reaction product OH-BTS.

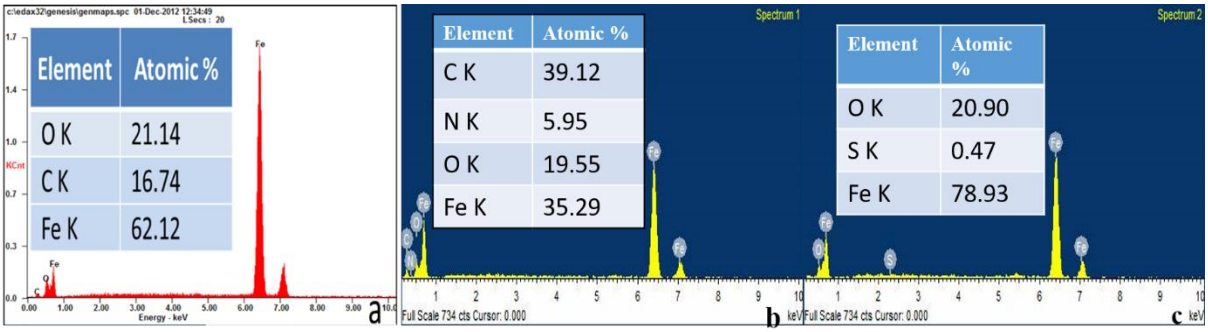

Fig. 3.8. EDX spectra for the worn surface of tested specimen balls lubricated with (a) PO, (b) OH-BT, (c) OH-BTS

3.4.5. Molecular Dynamics Simulation

Equilibration of the investigated models was carried out for 15 nanoseconds, and the next five nanoseconds was treated as the production run. **Fig. 3.9** shows configuration snapshots of the simulated system at the end of the production run. It can be seen that the conformation of the molecule after adsorption was different from the initial or starting conformation. The Figure shows the conformation of the additive molecule after adsorption on the adsorbent after hiding the solvent (alkane) molecules. However, there is a range of equilibrium conformations during the production run. Therefore, long time average radial distribution functions (RDF) have been used to understand the

interaction mechanism of the additive molecule with the adsorbent surface. Here RDF describes the probability of occurrence of a particular heteroatom at a given distance from the adsorbent surface Fe atom. The calculated RDF's are calculated from the time-average data obtained during the production run of the investigated systems.

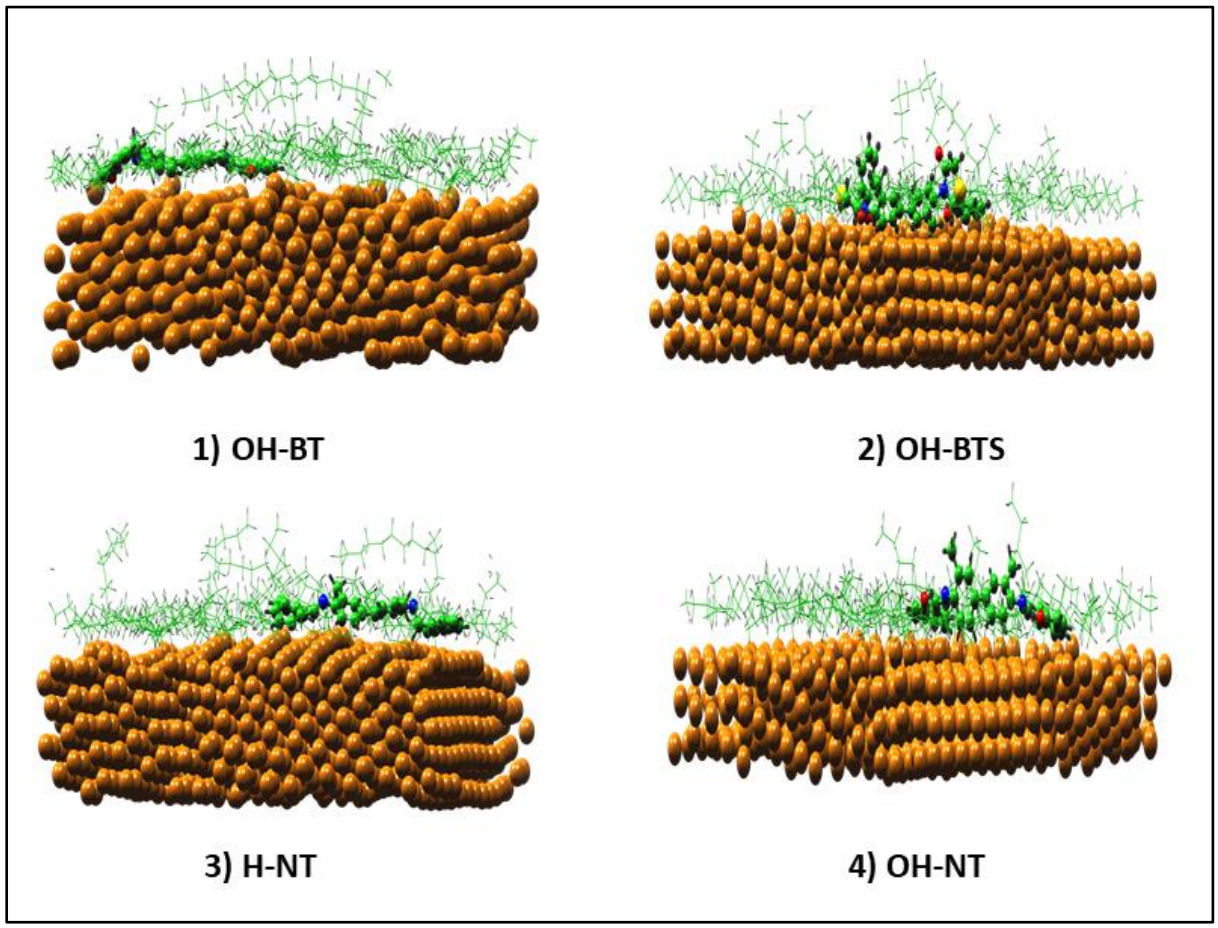

Fig. 3.9. Equilibrium adsorption configurations of the adsorbates on Fe (110) surface:

(1) OH-BT, 2) OH-BTS 3) H-NT 4) OH-NT [full view (with Paraffin oil)]

(colour represents in the structure as green: carbon, black: hydrogen, yellow: sulphur, dark yellow: iron, blue: nitrogen, red: oxygen)

Fig. 3.10(a) presents the RDF of Fe of the adsorbent surface with the N (heteroatom) in the additive molecule. One can see that the first and the highest peak is

obtained at (the closest) distance (3.0 to 3.25Å) for r(Fe(M) – N(OH-BT)). The symbol r(Fe(M) – N(OH-BT)) represents the variation of the g(r) function with the distance between Fe and N (of OH-BT). Only the first peak is considered in the present discussion since subsequent peaks take Fe atoms below the first layer (or nearest interaction) into account for calculating the g(r). The next highest peak is observed for r(Fe(M) – N(OH-NT)) at ~ 3.25Å. Although the r(Fe(M) – N(OH-NT)) peak maximum occurs at the same distance, its intensity is lesser than the OH-BT peak. Finally, the first peak of r(Fe(M) – N(OH-BTS)) is seen around ~3.5 – 3.75Å.

Fig. 3.10(b) presents the RDF's between adsorbent Fe and O atom in the additive molecule. Since O atom is not present in the H-NT additive, therefore, no RDF could be plotted for this case. Thus, only three plots are seen in Figure 10b. The highest first peak is obtained for r(Fe(M) – N(OH-BT)) in the ~ 2.75 – 3.25 Å range. The first peaks for r(Fe(M) – O(OH-BTS)) and r(Fe(M) – O(OH-NT)) are also observed in the same range. However, their intensities are much lesser than that of r(Fe(M) – N(OH-BT)). Moreover, r(Fe(M) – O(OH-BTS)) and r(Fe(M) – O(OH-NT)) peaks have similar heights.

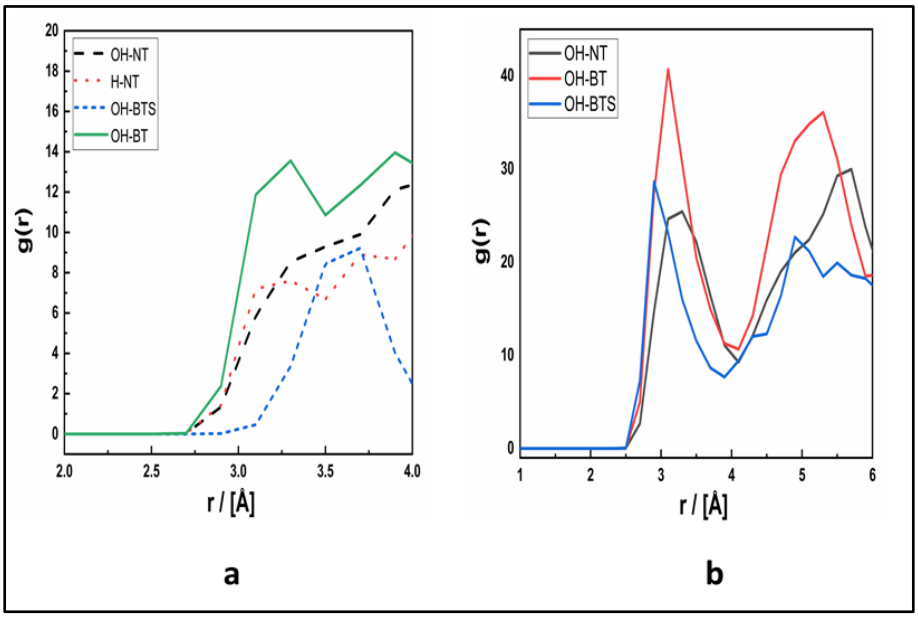

Fig. 3.10 (a) Radial distribution function of nitrogen atoms of Schiff bases with an iron atom at distance r.

(b) The radial distribution function of oxygen atoms of Schiff bases with an iron atom at distance r.

Therefore, it can be concluded that OH-BT interacts through its heteroatoms and these interactions are stronger than those of OH-NT. In turn, OH-NT displays stronger interaction between Fe and N (of the additive molecule) than for OH-BTS. The strength of the interaction between Fe and O (in the additive molecule) is similar for OH-NT and OH-BTS. Overall OH-NT displays better adsorption on the Fe adsorbent (than OH-BTS) because of its stronger Fe – N interaction. The first peak of r(Fe(M) – N(H-NT)) occurs at nearly the same distance as that of OH-NT, but it is slightly lower in intensity. However, H-NT does not have an O atom. Therefore, the interaction due

to O is missing. Owing to this, H-NT displays the weakest adsorption behavior on the Fe adsorbent and consequently the highest wear rate.

3.5. Conclusions

The synthesized Schiff bases derived from *o*-tolidine behaved as wear and friction modifier in paraffin oil at very low concentration, 0.25% w/v. Order of their efficiency was found to lie in the following descending order:

- OH-BT > OH-NT > H-NT > ZDDP > PO

The reference additive ZDDP shows good results at much higher concentration, 1% w/v as reported in our earlier communications. Besides this, ZDDP is not environment-friendly having high SAPS content due to two sulfur and two phosphorus atoms and an additional zinc atom in its structure. Load- carrying ability of paraffin oil was fairly enhanced in case of different admixtures and followed the same order as that of antiwear efficiency. The overall, running -in and steady-state wear rates were found to be maximum for plain paraffin oil. These were tremendously reduced when its blends with additives were used for lubrication. The extent of reduction in wear rates in the presence of Schiff bases is appreciably compatible with their corresponding tribological data. Morphology of worn surface of wear scar in the presence and absence of additives studied by SEM and AFM correlate very well with the antiwear behavior. Schiff base is supposed to be adsorbed on the metal surface by its characteristic imine group. When imine group turns into single C-N bond in the reaction product OH-BTS, antiwear properties were dramatically reduced. The reduction in antiwear properties could be related to the non-planar conformation of this molecule after its adsorption on to the iron surface as revealed by MD simulation results. Mechanism of action of additives

has been proposed based on the RDF (concerning additive heteroatoms) obtained from molecular dynamics simulation studies. It appears that adsorption of the additive molecules occurs mainly by the Fe – N and Fe – O interactions. These interactions are strongest for the OH-BT additive, which also displays the best adsorption and lowest wear rate properties.